

Early snowmelt events: detection, distribution, and significance in a major sub-arctic watershed

This content has been downloaded from IOPscience. Please scroll down to see the full text.

2013 Environ. Res. Lett. 8 014020

(<http://iopscience.iop.org/1748-9326/8/1/014020>)

View [the table of contents for this issue](#), or go to the [journal homepage](#) for more

Download details:

IP Address: 128.131.44.44

This content was downloaded on 29/11/2016 at 13:41

Please note that [terms and conditions apply](#).

You may also be interested in:

[Recent ice cap snowmelt in Russian High Arctic and anti-correlation with late summer sea ice extent](#)
Meng Zhao, Joan Ramage, Kathryn Semmens et al.

[Assessment of spring floods and surface water extent over the Yamalo-Nenets Autonomous District](#)
A M Trofaier, A Bartsch, W G Rees et al.

[Detection of the timing and duration of snowmelt in the Hindu Kush-Himalaya using QuikSCAT, 2000–2008](#)
Prajwal K Panday, Karen E Frey and Bardan Ghimire

[Surface water inundation in the boreal-Arctic: potential impacts on regional methane emissions](#)
Jennifer D Watts, John S Kimball, Annett Bartsch et al.

[Satellite microwave remote sensing of North Eurasian inundation dynamics: development of coarse-resolution products and comparison with high-resolution synthetic aperture radar data](#)
R Schroeder, M A Rawlins, K C McDonald et al.

[Methane emissions from western Siberian wetlands: heterogeneity and sensitivity to climate change](#)
T J Bohn, D P Lettenmaier, K Sathulur et al.

[Multi-temporal image analysis of historical aerial photographs and recent satellite imagery reveals evolution of water body surface area and polygonal terrain morphology in Kobuk Valley National Park, Alaska](#)
Marius Necsoiu, Cynthia L Dinwiddie, Gary R Walter et al.

[New satellite climate data records indicate strong coupling between recent frozen season changes and snow cover over high northern latitudes](#)
Youngwook Kim, J S Kimball, D A Robinson et al.

Early snowmelt events: detection, distribution, and significance in a major sub-arctic watershed

Kathryn Alese Semmens¹, Joan Ramage¹, Annett Bartsch^{2,3} and Glen E Liston⁴

¹ Earth and Environmental Sciences Department, Lehigh University, 1 West Packer Ave, Bethlehem, PA 18015-3001, USA

² Department of Geodesy and Geoinformation, Vienna University of Technology, Gusshausstrasse 27-19, A-1040 Vienna, Austria

³ Austrian Polar Research Institute, Vienna, Austria

⁴ Cooperative Institute for Research in the Atmosphere, Colorado State University, Fort Collins, CO 80523-1375, USA

E-mail: kalese@gmail.com

Received 19 September 2012

Accepted for publication 22 January 2013


Published 12 February 2013

Online at stacks.iop.org/ERL/8/014020

Abstract

High latitude drainage basins are experiencing higher average temperatures, earlier snowmelt onset in spring, and an increase in rain on snow (ROS) events in winter, trends that climate models project into the future. Snowmelt-dominated basins are most sensitive to winter temperature increases that influence the frequency of ROS events and the timing and duration of snowmelt, resulting in changes to spring runoff. Of specific interest in this study are early melt events that occur in late winter preceding melt onset in the spring. The study focuses on satellite determination and characterization of these early melt events using the Yukon River Basin (Canada/USA) as a test domain. The timing of these events was estimated using data from passive (Advanced Microwave Scanning Radiometer—EOS (AMSR-E)) and active (SeaWinds on Quick Scatterometer (QuikSCAT)) microwave remote sensors, employing detection algorithms for brightness temperature (AMSR-E) and radar backscatter (QuikSCAT). The satellite detected events were validated with ground station meteorological and hydrological data, and the spatial and temporal variability of the events across the entire river basin was characterized. Possible causative factors for the detected events, including ROS, fog, and positive air temperatures, were determined by comparing the timing of the events to parameters from SnowModel and National Centers for Environmental Prediction North American Regional Reanalysis (NARR) outputs, and weather station data. All melt events coincided with above freezing temperatures, while a limited number corresponded to ROS (determined from SnowModel and ground data) and a majority to fog occurrence (determined from NARR). The results underscore the significant influence that warm air intrusions have on melt in some areas and demonstrate the large temporal and spatial variability over years and regions. The study provides a method for melt detection and a baseline from which to assess future change.

Keywords: snowmelt, passive microwave, active microwave, rain on snow, remote sensing, cryosphere

 Online supplementary data available from stacks.iop.org/ERL/8/014020/mmedia



Content from this work may be used under the terms of the [Creative Commons Attribution-NonCommercial-ShareAlike 3.0 licence](http://creativecommons.org/licenses/by-nc-sa/3.0/). Any further distribution of this work must maintain attribution to the author(s) and the title of the work, journal citation and DOI.

1. Introduction

Alaskan winters have warmed by 3.5°C over the past 50 years, almost twice that of the annual average temperature

increase (Karl *et al* 2009). Observations and climate models have found greater warming in winter, and projections suggest changes in winter will continue (Hay and McCabe 2010). The late winter and early spring period in the Arctic is significant due to its control on the initiation of ecological and hydrological processes and shifts to earlier melt and green-up dates are already being experienced and expected in the future (Serreze *et al* 2000, Cayan *et al* 2001, Stone *et al* 2002, Schwartz *et al* 2006, Wang *et al* 2011). Additionally, the late spring is important for surface energy budgets because of changes in albedo and solar radiation that result in higher outgoing shortwave radiation than other seasons and for the large amounts of latent heat required to melt snow (Male and Granger 1981, Cohen 1994). Of particular significance during this period are *early melt events*, defined here as short-lived melt events detected with remotely sensed passive microwave brightness temperatures that occur before the relatively continuous spring melt onset. A typical seasonal sub-arctic snow cycle starts with snow fall and accumulation throughout late fall and winter until temperatures rise and are consistently around or above the freezing point in mid to late spring when the snowpack melts during the day and refreezes at night when temperatures drop. This usually lasts for several days to weeks until temperatures at night are higher and the snowpack becomes isothermal, saturated and actively melts day and night until the surface is snow free. Early melt events occur before this melt cycle begins in the spring and are much shorter events (one or a few days), usually a result of brief warm temperatures, warm moist air (fog) or rain on snow.

While developing an algorithm for determining the spring melt onset with passive microwave data, the earlier, short term events were noticed and hypothesized to impact the structure of the snowpack, create ice lenses, and affect melt runoff. However, little is known of the events' characteristics or effects, leading to such questions as: what are the influencing or causative factors? Are these events increasing in number, area, and frequency? What is their spatial and temporal variability? In order to investigate these questions, we considered satellite detected early melt events for the Yukon River Basin for the period 2003–2009. We utilized multiple datasets (ground station data, model data, and remote sensed data) in order to validate the detections, as well as to explore possible causes. Results illustrate the spatial and temporal variability of melt events and highlight the need for future study on the significance of the effects of these events, especially with increasing temperatures amplifying changes in late winter when these events tend to occur.

It is hypothesized that the satellite detected melt events can be explained by rain on snow (ROS), melt from warm air mass intrusions resulting in positive net turbulent flux, or melting of the snowpack due to temperature and radiative heating. ROS events have previously been investigated in the literature and found to have significant biological, hydrological, and ecological impacts (Putkonen and Roe 2003, Ye *et al* 2008, Grenfell and Putkonen 2008, Rennert *et al* 2009, Bartsch *et al* 2010, Hansen *et al* 2011). Biologically, ROS events can result in ungulate (caribou, musk oxen, reindeer) mortality because the ability

to effectively forage is impeded by ice layers that can require costly energy expenditures (Aanes *et al* 2000, Grenfell and Putkonen 2008, Putkonen *et al* 2009, Rennert *et al* 2009). Hydrologically, rain on snow can lead to severe flooding. The ice layers serve as impediments that double snowpack storage capacity (liquid water holding capacity is about 14.2% near ice layers compared to an average capacity of 6.8%) and the snowpack's high conductivity (due to saturation and preferential flow paths) produces high discharge (Singh *et al* 1997). The latent heat carried by rain not only heats snow and creates melt, it also raises the underlying soil temperature impacting the permafrost heat budget (if the amount of rain is large enough) due to the reduction of the insulative properties of the snowpack (Putkonen and Roe 2003, Grenfell and Putkonen 2008, Rennert *et al* 2009, Westermann *et al* 2011). This modification of winter soil temperature may have consequences for the annual hydrological cycle (Grenfell and Putkonen 2008) and may have long-lasting impacts on permafrost degradation and maximum thaw depth (Westermann *et al* 2011).

Ecologically, ROS events have been found to be a significant source of stream $\text{NO}_3\text{-N}$ during the winter, resulting in acidic downstream waters impacting aquatic biota and in recent years, the portion of the annual $\text{NO}_3\text{-N}$ export has increased (Eimers *et al* 2007). This coincides with an increase in frequency and extent of ROS occurrences in many Arctic and sub-arctic areas (Rennert *et al* 2009, Bartsch *et al* 2010, Liston and Hiemstra 2011). Liston and Hiemstra (2011) modeling results of domain averaged trends in the past 30 years (1979–2009) found decreasing snow and increasing rain on snow throughout the Arctic, with rain on snow days increasing by 0.03 days per decade, total snow days decreasing 2.49 days per decade, and air temperature (with snow on the ground) increasing by 0.17 °C per decade. As air temperatures increase in the future, ROS events are projected to be more frequent, have a wider spatial extent, and become common in areas they are now rare (Ye *et al* 2008, Rennert *et al* 2009, Hansen *et al* 2011). A typical global climate model scenario projects a 40% increase in the area affected by ROS by 2080–2089, driven by winter warming and trends toward positive North Atlantic Oscillation (NAO) phase associated with warm air incursions (Putkonen and Roe 2003).

The significant effects of and the projected future increase in ROS events motivate research into their causes and characteristics, however, studying ROS events is challenging due to their sporadic occurrence, and the need for consistent and wide coverage meteorological data and accurate rain and snow measurements (Grenfell and Putkonen 2008). While most evidence is anecdotal, several studies have attempted to characterize ROS events using station data, reanalysis datasets, and climate models (Rennert *et al* 2009). There are disadvantages to each approach including sparse coverage, difficulty in determining precipitation in cold regions, and spatial resolution and scale issues (Rennert *et al* 2009).

Satellite data have also been used; specifically, Grenfell and Putkonen (2008) used Special Sensor Microwave Imager (SSM/I) data and an emissivity model to detect the stages of ROS with spectral gradients and polarization ratios. The

ROS events were characterized by a low gradient ratio and large polarization ratio compared to the normal snowpack conditions (Grenfell and Putkonen 2008). During the ROS event, a rapid change in emissivity and temperature occurs initially and is followed by the freezing of liquid with a persistent T_b signature from the formation of ice layers and grain size change that may last until melt onset in the spring (Grenfell and Putkonen 2008).

Though similar to Grenfell and Putkonen (2008)'s previous study, the research presented here utilizes higher resolution passive microwave data from the Advanced Microwave Scanning Radiometer—Earth Observing System (AMSR-E) which has 12.5 km spatial resolution compared to SSMI's 25 km. In addition, the algorithm and method for melt detection differs between the two studies; here detection depends on melt thresholds and diurnal amplitude variation changes in conjunction with a backscatter change detection approach using QuikSCAT active microwave data, while Grenfell and Putkonen (2008) utilize a ratio approach. Further, our study strives to provide a better understanding of all early melt events (not just ROS), providing a spatially and temporally distributed picture of the variability and significance of these events across the Yukon River Basin in Alaska.

Better characterization of early melt events and ROS is important for improving modeling and algorithm performance. Streamflow and flood prediction may be improved through the estimation of timing and volume of runoff from ROS events (Singh *et al* 1997, McCabe *et al* 2007). Runoff from the snowpack is affected by surface melt, movement of water through the pack (preferential flow paths), infiltration into the soil, overland flow, and snow metamorphism (Singh *et al* 1997). The transit time from melt at the surface to the base of the pack can be estimated from simple continuity reasoning, however, meltwater flux moves more slowly when refreezing has taken place (Bengtsson 1982), a significant consideration for modeling of runoff. Although ROS events are more likely to cause severe flooding than short melt events induced radiatively (Kattelmann 1985), melting of the snowpack without ROS also has significant effects, changing the structure of snowpack stratigraphy and volume storage capacity, possibly affecting runoff dynamics. Additionally, the operational algorithms for passive microwave satellite data products (snow water equivalent) may be impacted by melt events in mid-winter and should be considered (Rees *et al* 2010).

2. Study area

The analysis focuses on the Yukon River Basin (YRB) for the time period 2003–9 when both AMSR-E and QuikSCAT data are available. The YRB (figure 1) is one of the largest basins in North America; it drains 853 300 km² and stretches from northwestern Canada through central Alaska, covering several ecoregions and land cover types, and encompasses a range of elevations (Brabets *et al* 2000). The majority of the basin can be characterized by a sub-arctic nival regime with snowmelt driving runoff (Brabets *et al* 2000, Woo *et al*

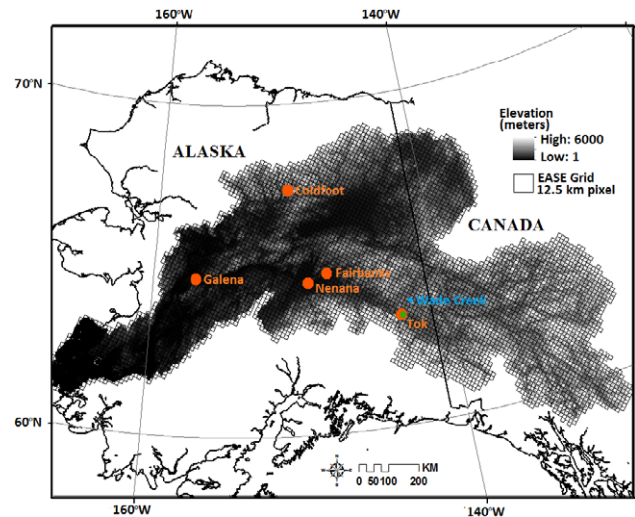


Figure 1. Overview of the Yukon River Basin study area with elevation and EASE-grid. Locations of ground station sites mentioned in the text are marked with orange circles. The pixel illustrated in figure 2 at Tok is marked green and the hydrological data used in figure 2 comes from Wade Creek marked blue. Topographic data (1:250 000 scale) is from Long and Brabets (2002).

2008). For the YRB, future climate modeling studies suggest earlier snowmelt timing of longer duration, the largest positive temperature changes in winter, and increased runoff with the largest changes in May, June, and July (Hay and McCabe 2010). Given the projections for significant change in the critical time of late winter prior to melt onset, the YRB is an ideal study area for focusing on the occurrence and variability of early melt events.

3. Data and methods

To detect and validate events, several datasets were utilized, including passive and active microwave data, model output from SnowModel (Liston and Hiemstra 2011), variables from the National Centers for Environmental Prediction (NCEP) North American Regional Reanalysis (NARR) (Mesinger *et al* 2006), and weather station data for some specific sites.

3.1. Passive microwave data

Brightness temperature (T_b) data from the Advanced Microwave Scanning Radiometer—Earth Observing System (AMSR-E) on the Aqua satellite (Ashcroft and Wentz 2006) was used to determine when and where surface melt occurred. Water in the snowpack increases the emissivity which results in a significant difference in T_b between wet and dry snow (Chang *et al* 1976, Ulaby *et al* 1986). Further, the bulk permittivity of snow is modified by rain on snow, resulting in a change in T_b that can be measured by passive microwaves (Grenfell and Putkonen 2008). Using the 36.5 GHz vertical channel due to its sensitivity to snow wetness (Ramage *et al* 2006) and relatively higher spatial resolution (14 × 8 km² resolution which is gridded as 12.5 km pixels in

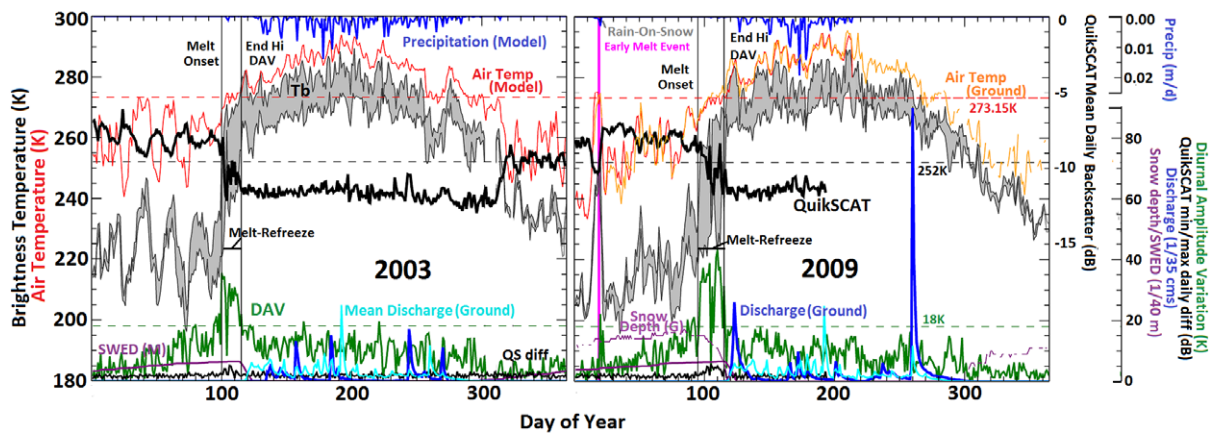


Figure 2. Time series of multiple datasets for a 12.5 km EASE-grid pixel encompassing Tok, Alaska (63.3216°N, 143.109°W). Left panel shows 2003—a year when there were no early melt events. Right panel shows 2009—a year of a rain on snow associated early melt event (pink vertical line). AMSR-E brightness temperatures are shaded gray and diurnal amplitude variation green. Solid black line is the mean daily backscatter (dB) from QuikSCAT and the thin bottom black line is the daily difference in minimum and maximum backscatter. Precipitation (top blue), air temperature (red), and SWE depth (dark purple) are from SnowModel. Air temperature (orange) and snow depth (light purple) are from the USDA Natural Resources Conservation Service Soil Climate Analysis Network (SCAN). Discharge (bottom dark blue with mean as cyan) is from Wade Creek Tributary near Chicken site 15320100 (see figure 1). Melt timing parameters (onset, melt–refreeze, end of high DAV) are shown with vertical black lines and labels.

the NSIDC Equal-Area Scalable Earth (EASE) grid), melt onset was determined as the first date when T_b was greater than 252 K and the diurnal amplitude variation (DAV), or difference between the ascending and descending passes, was greater than 18 K for three of five consecutive days. These thresholds have been previously determined and validated in the YRB (Apgar *et al* 2007). Typically melt onset is followed by a period of high DAV where the snowpack is melting during the day and refreezing at night. At the end of this melt–refreeze period, or high DAV, the snowpack may be actively melting both day and night until snow disappearance. Figure 2 illustrates these melt timing parameters.

For early melt event detection, the time period of analysis was constrained to between the first of the year and the melt onset date derived from the passive microwave data (described in the section above). Similar to the melt onset determination, early melt events were defined when the T_b was greater than 252 K and DAV was greater than 10 K. A lower DAV threshold (10 K) was employed for the early melt event detection because visual inspection of the data showed some definitive events were missed due to the DAV threshold being too high (supplementary material, figure S1 available at stacks.iop.org/ERL/8/014020/mmedia). Other algorithms were tested but not used, including utilizing the 18.7 GHz wavelength (more sensitive to deeper melt infiltration and noisier than 36.5 GHz in the DAV signal), as well as a single channel polarization difference previously suggested for the detection of ice lenses (Rees *et al* 2010).

3.2. Active microwave data

Melt events prior to melt onset (the start of the melt–refreeze period leading to continuous melt) were also determined from the active microwave sensor SeaWinds on QuikSCAT (13.4 GHz, Ku-band). SeaWinds scatterometer data (Jet

Propulsion Laboratory) were processed and gridded to a 12.5 km regular grid as described in Kidd *et al* (2003, 2005), Bartsch *et al* (2007, 2010). An increase in backscatter reflects a refreezing/icing event, while surface melt results in a drop in backscatter up to −6 decibels (dB) (Bartsch *et al* 2010). Given these characteristics, a change detection approach considers days before and after the event. Specifically, a date was determined as a thaw and refreeze event when the difference in the mean daily backscatter of the three days before and after the date exceeded 1.5 dB, a threshold previously validated from ground observations on Yamal Peninsula, Russia, as explained in Bartsch *et al* (2010). Wilson *et al* (2012) successfully used this methodology to determine frequency and extent of icing/thaw–refreeze events across Alaska.

3.3. Passive and active microwave data

In this study early melt events were detected using both the AMSR-E detection algorithm (section 3.1) and the QuikSCAT change detection algorithm (section 3.2). Specifically, the QuikSCAT freeze–thaw detections were used to validate and filter the AMSR-E detected events⁵, so that the determination of an early melt event occurred when both sensors’ thresholds were met. Due to this combination of the passive and active sensors, the early melt events results should be viewed as conservative estimates. QuikSCAT is highly sensitive to snow wetness and can map actively melting areas, while AMSR-E (at 36.5 GHz) is sensitive to surface melt and distinguishes between dry and wet snow (Foster *et al* 2011). Both sensors were used in this study to provide more confidence in the detection of melt events. Because the AMSR-E DAV threshold was lowered (to 10 K from 18 K) in order to make

⁵ See supplementary material (figures S2–S4 available at stacks.iop.org/ERL/8/014020/mmedia) for a comparison of the early melt detections between AMSR-E and QuikSCAT.

the algorithm more sensitive for detecting the short, early melt events, there resulted in an overestimation of events which was countered by also requiring the QuikSCAT detection to be met. Refer to the supplementary material (available at stacks.iop.org/ERL/8/014020/mmedia) for more on the comparison between the two sensors. Previous studies have used QuikSCAT and AMSR-E data to complement each other for melt onset detection in order to reduce uncertainty and improve detection of snow cover and melt (Foster *et al* 2011). Combining AMSR-E and QuikSCAT has also been found to improve sea ice mapping (Yu *et al* 2009).

3.4. Model derived snow dataset

Detected early melt events were compared with air temperature (2 m), precipitation, and snow water equivalent (SWE) depth spatially distributed variables from the dataset derived from the SnowModel and MicroMet modeling system described in Liston and Hiemstra (2011). This is a physically based model that relies on topographic data (1 km DEM), land cover data (hybrid dataset of GlobCover and Circumpolar Arctic Vegetation Map), and atmospheric forcing data (NASA Modern Era Retrospective-Analysis for Research and Applications or MERRA) (Liston and Hiemstra 2011, and references therein). Rain on snow (ROS) is generated as a secondary product from the primary data fields. The model derived variables are on a 10 km grid, a finer resolution than typical climate models, allowing for snow evolution process representation to be improved. This grid resolution is also relatively comparable to the EASE-grid scale used to map the AMSR-E data (12.5 km). SnowModel has been previously authenticated and there is confidence in the representativeness of the simulated snow data products (Liston and Hiemstra 2011). The model is used here for validation and attribution of the satellite detections of melt and is viewed as a conservative estimate of rain on snow.

3.5. NCEP North American Regional Reanalysis (NARR)

NCEP NARR data, including air temperature (2 m), dew point temperature, visibility, and relative humidity, were used to determine the occurrence of fog. Fog was defined when the difference between air temperature and dew point temperature was less than 2.5 °C, or when relative humidity was greater than 98%, or when visibility was less than 1000 km (AMS 2000, OFCM 2005). NARR data are on a 349 × 277 (0.3° or 32 km) grid and were re-sampled (nearest neighbor technique) to the 12.5 km EASE-Grid to compare to the AMSR-E data.

The relatively moister and warmer conditions forming fog are considered to affect snow and melting. Snowmelt is accelerated with condensation melt associated with warm, moist air mass intrusions that result in higher melt rates than those produced from radiation or sensible heat alone (Zuzel *et al* 1983). Additionally, snowmelt during ROS is sensitive to net turbulent flux (sensible and latent heat flux) which provides over three-fourths of the energy for snowmelt (Marks *et al* 1998). Condensation on the snow surface from high humidity, air temperatures, and winds results in enhanced snowmelt (Marks *et al* 1998).

3.6. Meteorological and hydrological data

Meteorological and hydrological data for several pixels were used to validate early snowmelt detection and model results. Temperature, precipitation, and snow depth variables were obtained from the National Climate Data Center's global summary of the day data for several sites, including Coldfoot, Galena, Nenana, and Fairbanks, Alaska. Air temperature and snow depth for some sites (Tok) are from the USDA Natural Resources Conservation Service Soil Climate Analysis Network (SCAN). Discharge data were obtained from the USGS National Water Information System. The available data were compared to time series of satellite brightness temperatures and backscatter and the detections of melt. For example, some stations had precipitation and snow depth allowing melt events detected by satellite to be corroborated with rain on snow. Only Tok and Galena data are shown in the results section in the interest of space.

3.7. Data limitations and uncertainties

There are several limitations and uncertainties to consider in the datasets utilized in this study. The remote sensing data products are limited by spatial resolution and scale issues. There is considerable sub-grid variability within a pixel footprint for both sensors. Since the interest of the study is the timing of melt and the signal is significant and distinct in both the emissivity increase (for passive microwave sensors) and backscatter drop (for active microwave sensors), the determination of melt timing is assumed to have a large signal to noise ratio enabling adequate detection amid contributions from sub-grid variability due to vegetation and topography. However, these factors do contribute some uncertainty to the datasets. Noise contributed from the instrument, azimuth effects, irregular sampling, and land cover heterogeneity are in general minimal for the QuikSCAT backscatter signal (Bartsch *et al* 2007). Differing overpass times are assumed negligible since data from QuikSCAT is a daily average of multiple retrievals and data from AMSR-E is averaged to two daily averages (one for morning and night) to calculate DAV. Additionally, while the original gridded data for each of the datasets is relatively similar (10 km for SnowModel and 12.5 km for AMSR-E and QuikSCAT) there is uncertainty introduced when scaling to the 12.5 km grid utilized for the analysis. Uncertainty is also introduced when comparing a single point ground station data to a 12.5 km pixel. The ground station and SnowModel datasets in general agree well, especially with regard to air temperature and presence of snowpack. SnowModel was rigorously validated against multiple data sources and found to be a good representation of the Arctic climatology (Liston and Hiemstra 2011). However, these SnowModel simulations do have some limitations including assumptions of static vegetation distribution and one way atmospheric forcing, as well as not including blowing snow processes. The NARR dataset represents an improved depiction of hydrology and land-atmosphere interaction compared to other reanalyses, because of its more accurate forcings to the land surface model, higher resolution, and

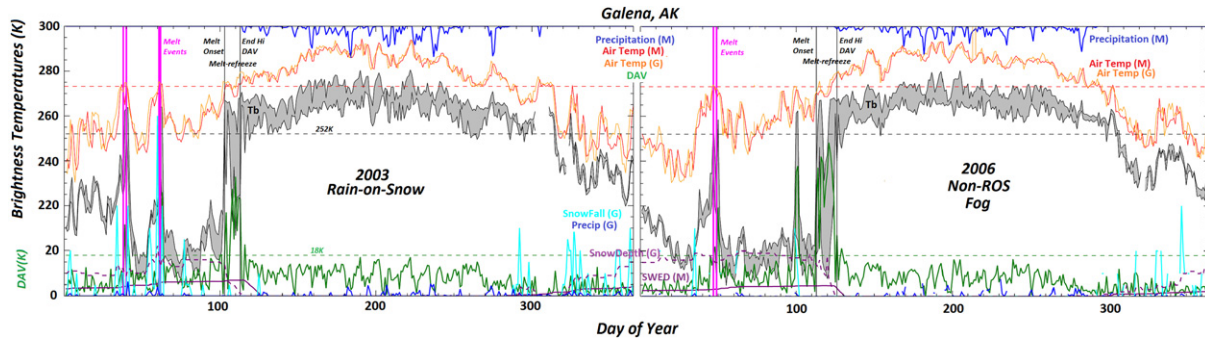


Figure 3. Time series of multiple datasets for a 12.5 km EASE-grid pixel encompassing Galena, Alaska (64.7406°N, 156.8856°W) for 2003 (left) a year with two early melt events associated with rain on snow as corroborated by ground station data of precipitation (bottom dark (rain) and light (snow) blue) and snow depth (bottom dashed purple line) and for 2006 (right) a year with one early melt event associated with fog (no rain on snow). Ground station data is from the Global Historical Climatology Network—Daily (USC00503212). Brightness temperature is shaded gray, DAV is green, air temperature from SnowModel is red and from ground station data is orange, precipitation from SnowModel is top blue line, SWE depth from SnowModel is bottom solid purple line. Early melt events are pink lines and melt timing (onset and refreeze) are black, labeled vertical lines.

direct assimilations of variables such as radiance (Mesinger *et al* 2006). However, like all (re)analysis products it is limited by its numerical approximations of physical and dynamical processes and the data it assimilates.

4. Results

To illustrate the occurrence and validity of early melt events, time series of several of the datasets used in this study are shown in figure 2 for 2003 and 2009 for a pixel encompassing Tok, Alaska where meteorological and hydrological data were available. Both QuikSCAT and AMSR-E detected an early melt event around January 19 (day 19) in 2009 while there was no early melt event in 2003. The 2009 melt event coincided with a rain on snow occurrence in SnowModel and above freezing air temperature data from the SCAN site at Tok. Of note is the increase in discharge relative to the mean immediately after the end of the associated high DAV (green line) in 2009 which is not seen in 2003. Early melt events or ROS events were not found for this pixel in the other years investigated (2004–2008). Compared to 2003, 2009 had a longer melt–refreeze period (20 days compared to 13 in 2003), primarily a result of the melt onset date being earlier (day 95 compared to day 100 in 2003). The end of melt–refreeze is relatively the same (115 for 2009 and 113 for 2003). In 2003, there were several periods of warmer temperatures prior to melt onset that were not significant enough to meet the melt thresholds. It should be noted that the air temperatures are daily averages at the 2 m level and so are not an exact (but rather a proximate) indication of surface temperatures.

To show further validation of the satellite detected melt events, figure 3 shows time series of brightness temperatures and ground station data for a pixel that encompasses Galena, Alaska. The ground station data corroborate two melt events detected by the sensor in 2003 as rain on snow. In 2006, a satellite detected melt event was not associated with rain on snow and most likely was due to fog or a warm air mass in the area. SnowModel matched the ground and satellite results

in 2006 but not in 2003, highlighting the utility of combining approaches rather than just relying solely on one or the other. Other ground station locations were investigated (see figure 1 for locations) but the results are similar and not shown in the interest of space.

Following the multiple dataset and pixel validation of the early melt event algorithm, the algorithm was applied to the entire Yukon River basin to observe the spatial and temporal variation of early melt days. Figure 4 shows the range of early melt days for 2008 and representative pixel time series for areas with a relatively large number of melt days (5–6) compared to a relatively small number of melt days (1–2) and to no early melt days. Early melt days appear to coincide spatially, reflective of synoptic atmospheric patterns. Areas closer to the ocean exhibit more melt variability before melt onset due to a milder, maritime climate. The same events can be seen in several of the pixels (notably figures 4(A)–(C)) but the occurrences are not always significant enough to represent actual melt in each place. It should be noted that the early melt event results are a conservative estimate due to the utilization of both the active and passive sensors.

To investigate the possible causative factors of the satellite detected early melt events, the events were first checked against ROS occurrences (from SnowModel), then fog occurrences (from NCEP NARR data), and all events, including the remaining events not explained by ROS and fog, were checked against above freezing temperatures (also from NCEP NARR). In 2009 (figure 5), 30% of the melt days coincided with ROS, while the rest were fog related (table 1). Those events not explained by ROS or fog corresponded to positive temperature days giving more confidence to the detection method and results since all the melt events were associated with above freezing temperatures. The proportion of events explained by ROS, fog, or positive temperatures varied considerably across years (figure 6). That said, there were some areas of consistent early melt event occurrence (figure 7), specifically the western end of the basin in the Innoko Lowlands comprised of substantial areas of

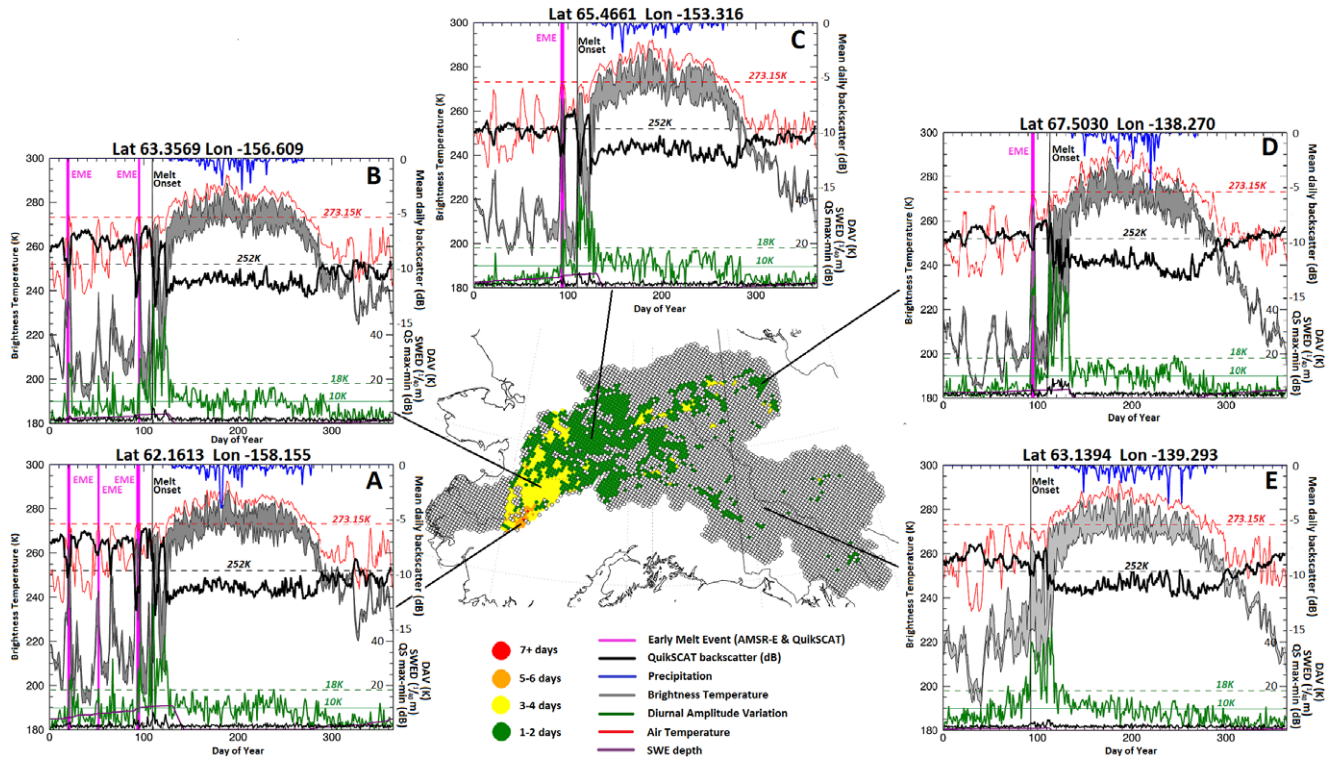


Figure 4. Number of early melt days detected by AMSR-E and QuikSCAT for 2008 across the Yukon River Basin (center) and select pixel time series of the various melt day categories (A)–(E). Time series show the brightness temperature min and max (gray shaded) with its threshold of 252 K (dashed gray line), the diurnal amplitude variation (bottom green line) with its threshold for melt onset of 18 K (dashed green line) and threshold for early melt events at 10 K (solid thin green line), the air temperature (red) with the 0° threshold (dashed red line), snow water equivalent depth (purple), and precipitation (upper blue line) from SnowModel. Early melt events (EME) (which can encompass multiple melt days⁶) are hot pink vertical lines and melt onset is demarcated with a vertical black line. QuikSCAT mean daily backscatter (dB) is the thick solid black line (right axis) and the difference between the minimum and maximum backscatter per day is shown at the bottom of each plot with the thin black line. Backscatter decreases coincide with T_b increases; both indicate melt. Panel (A) shows the orange category (5–6 days)—mostly broadleaf forest land cover, (B) shows the yellow category (3–4 days)—broadleaf and dwarf shrublands, (C) and (D) show the green category (1–2 days)—needleleaf and broadleaf forest, and (E) shows no days—needleleaf forest land cover.

Table 1. Number of pixels with early melt events (EME), the total number of early melt days for the year, the number and per cent of early melt days coinciding with rain on snow (ROS) and fog. The remaining events not explained by ROS or fog correspond with above freezing temperatures (last columns).

	Number of pixels with EME	Total number of detected EMEs	EME and ROS		EME and Fog		EME and Temp	
			Number	Per cent (%)	Number	Per cent (%)	Number	Per cent (%)
2003	1247	2123	416	20	390	18	1317	62
2004	228	287	28	10	169	59	90	31
2005	549	1035	76	7	666	64	293	28
2006	465	811	8	1	96	12	707	87
2007	311	405	140	35	174	43	91	22
2008	1483	2739	298	11	1436	52	1005	37
2009	1327	1645	497	30	1109	67	39	2

wetlands and flat river flood plains (Wahrhaftig 1965). Fog occurrences explained more events than ROS. In some years (2003 and 2008) ROS and fog did not explain many of the detected events (but all of the events including those unexplained by ROS and fog were associated with above freezing temperatures).

⁶ This is the reason why there appear to be fewer events (labeled with pink (E) then the color of the pixel (green, yellow, or orange). One event can represent multiple days of melt.

5. Discussion

The spatial and temporal occurrences of detected early melt events demonstrate the large variability associated with this phenomenon. Considerable spatial variation in ROS trends were also found by Liston and Hiemstra (2011). There are some areas of consistent occurrence toward the western end of the basin which may reflect the synoptic conditions of a more maritime climate and air mass patterns, or the characteristics

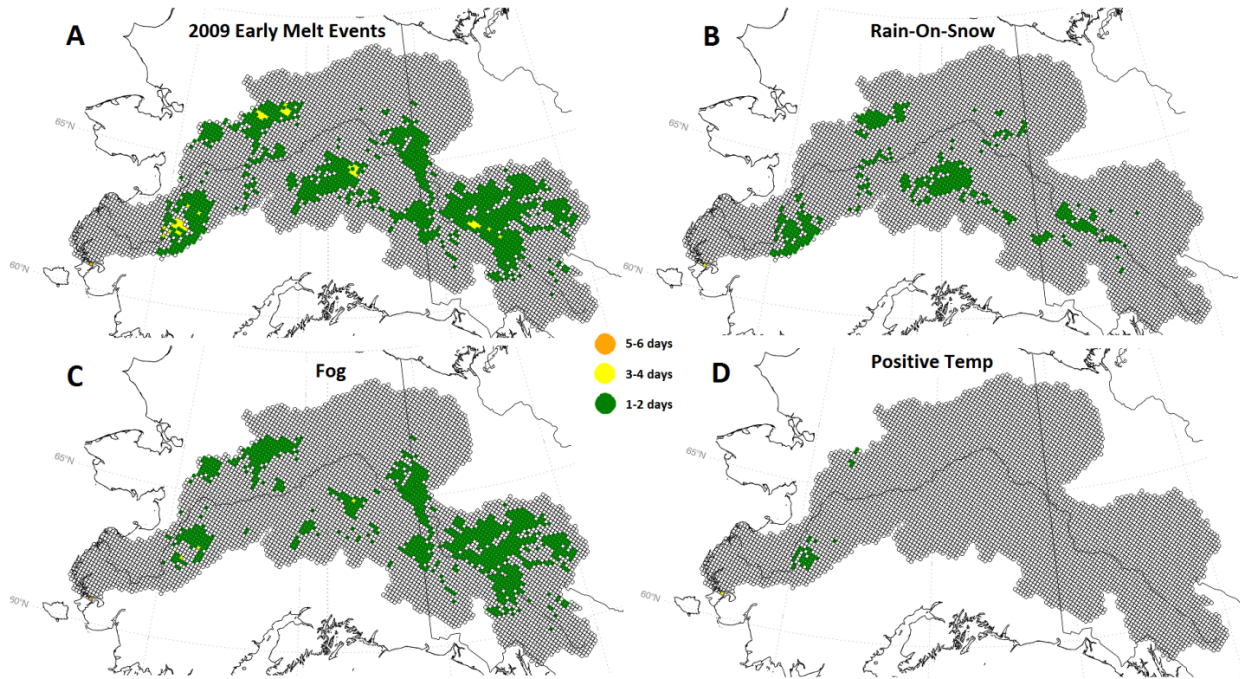


Figure 5. (A) Number of satellite (AMSR-E and QuikSCAT) detected early melt events for 2009 across the Yukon River basin with green showing 1–2 days, yellow 3–4 days, and orange 5–6 days; (B) number of the satellite detected events that coincide with rain on snow (ROS) from SnowModel; (C) number of satellite detected events coinciding with fog occurrence from NCEP NARR data; (D) the remaining (not associated with ROS or fog) satellite detected events which coincide with above freezing temperatures from NCEP NARR. For 2009, the majority of detected events are explained by ROS and fog.

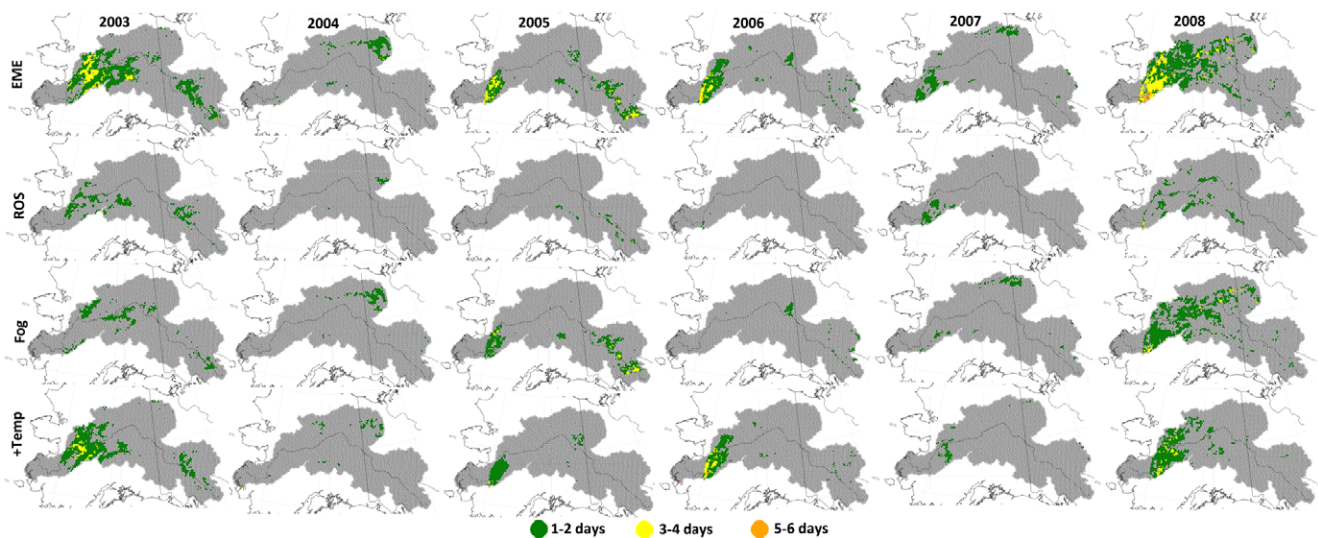


Figure 6. Temporal and spatial variability of the occurrence of early melt days for years 2003 through 2008: (top row) detected by satellite (AMSR-E and QuikSCAT); (second row) days coinciding with rain on snow (ROS) from SnowModel; (third row) days coinciding with fog occurrences; and (bottom row) remaining days not ROS or fog that are associated with above freezing temperatures.

of the land cover/ecoregion of the wetlands and flat flood plains of the Innoko Lowlands/Interior Bottomlands (Brabets *et al* 2000). Wilson *et al* (2012) also found frequent formation of ice layers in southwestern Alaska using QuikSCAT icing detections. Other studies have found ROS to be associated with southwesterly flow bringing warm air incursions, and upper level flow (represented with 500 hPa geopotential height field from ERA-40) to be better at characterizing

events than rain amounts (which tend to be underestimated) (Rennert *et al* 2009). ROS has been found to be associated with the Pacific-North American (PNA) pattern with the negative phase producing conditions likely to foster ROS events for Alaska (Rennert *et al* 2009). Further, ROS events in Spitsbergen have been linked to the North Atlantic Oscillation (NAO) when warm air incursions (prominent in the positive

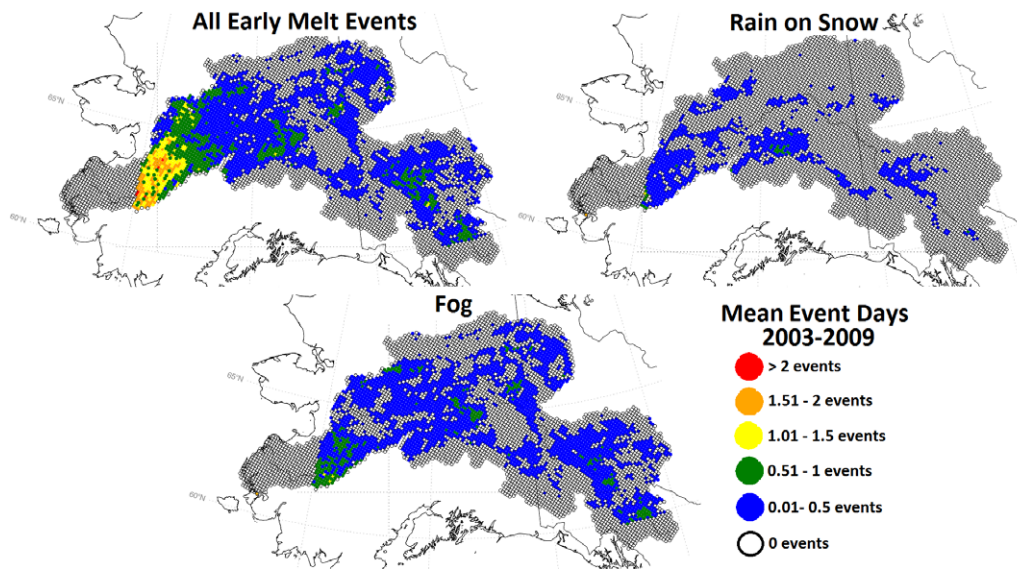


Figure 7. The mean number of early melt events for 2003–2009 as detected by both passive (AMSR-E) and active (QuikSCAT) satellite sensors, illustrating areas of consistent early melt occurrence.

phase of NAO) passed through the region (Putkonen and Roe 2003).

While radiation transfer and turbulent exchange (the sum of sensible and latent heat transfer) are the most important exchange processes governing energy interactions at the snow surface (Marks and Dozier 1992), terrain, air mass conditions, and time of year influence which process is more important (Male and Granger 1981). Usually, radiation dominates snowmelt under normal conditions but air mass intrusions (especially warm and wet) can influence the turbulent energy exchange bringing positive sensible heat flux and condensation on the snow surface, initiating snowmelt (Sverdrup 1936, Male and Granger 1981). Thus while sites may be similar physically, geographical differences such as which side of the mountain range or proximity to coast mean the sites will have different air mass intrusions and patterns, affecting the magnitude and relative importance of the energy fluxes (Male and Granger 1981). In this study, fog occurrence is viewed as a proxy for warm air mass intrusion which creates condensation on the snow surface resulting in melt that is detected by the passive microwave. The importance of these warm air intrusions is underscored by the relatively high percentage (table 1) and wide spatial distribution of early melt events that are explained by them.

The variability in causative factors of the melt events is a significant finding from this study. ROS was not the main influence for many of the years and areas, instead fog and positive temperatures largely coincided with and contributed to melt. This result highlights the benefit of utilizing remotely sensed brightness temperatures for detecting melt events. Satellite microwave data can provide near real-time information that is spatially continuous with high temporal resolution that is not affected by darkness or clouds. Relying solely on modeling results or weather station data fails to capture all melt events consistently since they can occur with

and without rain on snow. This conclusion is supported by the Banks Island case study where a severe ROS event in October 2003 resulted in 20 000 musk oxen deaths, but detection evidence based only on rain amounts would fail to garner significant attention (Grenfell and Putkonen 2008, Rennert *et al* 2009, Putkonen *et al* 2009). Additionally, the sparse network of weather observations in the Arctic and the lack of relevant information collected (i.e. the mixed fraction of rain and snow, not just total dominant precipitation) means ROS are likely underestimated (Grenfell and Putkonen 2008, Putkonen *et al* 2009).

Further, reliable detection of ROS with automated field equipment is a challenge due to complications from freezing water or melting snow (Putkonen *et al* 2009). As such, a critical need is field instrumentation that can detect melt events with high temporal resolution. Field data on the specific effects of melt events would further serve to address the current need for information on the storage capacity of snow throughout the various stages of metamorphosis and ice lens development, and the consequent effects on runoff (Singh *et al* 1997). It may also allow for the quantification of the amount of liquid water in the snow produced by a melt event that is detectable by satellite—a future direction for research. Early melt events may affect the structure and vertical compaction of the snowpack, number of ice lenses (layers), snowpack wetness, meltwater percolation, underlying soil temperatures, and runoff, thus continued study of their occurrence, effects, and trends is important.

6. Conclusions

An algorithm for detecting early melt events using passive and active microwave sensors was developed and validated against modeling results, reanalysis climate data, and ground based meteorological and hydrological data. Events were detected

by defining melt thresholds in passive microwave (AMSR-E) and active microwave (QuikSCAT) datasets. The spatial and temporal variability across the study area (Yukon River Basin) was considerable but there were a few consistent areas of occurrences, notably the wetlands/lowlands of the western end of the basin exhibiting a more maritime climate with frequent warm air mass intrusions. While some events can be explained by ROS events, many more coincide with fog occurrence which may reflect the influence of warm air mass advection. All events (those associated with ROS, fog, and those remaining) are associated with positive temperatures. ROS events may result in changes to hydrology, as seen in the increase in discharge relative to the mean for some pixels. The results suggest a practical methodology for detection of melt events, not confined to ROS, over wider spatial domains than currently possible with just sparse meteorological networks. The similar findings from the diverse data sources utilized in this study enhance the confidence in the results. The results also provide a baseline for assessing future change during the critical late winter/early spring period—a time of the year when increases in temperature and the resulting effects are projected to be enhanced in the future.

Acknowledgments

We appreciate data and model output from multiple sources: AMSR-E data was provided by the National Snow and Ice Data Center, SeaWinds QuikSCAT data are from the Jet Propulsion Laboratory, NASA, Pasadena, California, NCEP Reanalysis data were provided by the NOAA/OAR/ESRL PSD, Boulder, Colorado, USA, from their web site at www.cdc.noaa.gov/, and all meteorological data were provided by NOAA National Climate Data Center and USDA SCAN and SNOTEL programs. Hydrological were data provided by the USGS National Water Information System. We would like to acknowledge financial support from Lehigh University and NASA Headquarters under the NASA Earth and Space Science Fellowship—Grant NNX10AP14H.

References

Aanes R, Saether B E and Oritsland N A 2000 Fluctuations of an introduced population of Svalbard reindeer: the effects of density dependence and climatic variation *Ecography* **23** 437–43

American Meteorological Society (AMS) 2000 *Glossary of Meteorology* 2nd edn (New York: Allen Press)

Apgar J D, Ramage J M, McKenney R A and Maltais P 2007 Preliminary AMSR-E algorithm for snowmelt onset detection in subarctic heterogeneous terrain *Hydrol. Process.* **21** 1587–96

Ashcroft P and Wentz F 2006 *updated daily. AMSR-E/Aqua L2A Global Swath Spatially-Resampled Brightness Temperatures V002, 2003–2009* (Boulder, CO: National Snow and Ice Data Center. Digital Media)

Bartsch A, Kidd R A, Wagner W and Bartalis Z 2007 Temporal and spatial variability of the beginning and end of daily spring freeze/thaw cycles derived from scatterometer data *Remote Sens. Environ.* **106** 360–74

Bartsch A, Kumpula T, Forbes B C and Stammler F 2010 Detection of snow surface thawing and refreezing in the Eurasian Arctic

with QuikSCAT: implications for reindeer herding *Ecol. Appl.* **20** 2346–58

Bengtsson L 1982 Percolation of meltwater through a snowpack *Cold Regions Sci. Technol.* **6** 73–81

Brabets T P, Wang B and Meade R H 2000 Environmental and hydrologic overview of the Yukon River Basin, Alaska and Canada *USGS Water-Resources Investigations Report 99-4204* (Anchorage, AK: USGS)

Cayan D R, Kammerdiener S A, Dettinger M D, Caprio J M and Peterson D H 2001 Changes in the onset of spring in the western United States *Bull. Am. Meteorol. Soc.* **82** 399–415

Chang A T C, Gloersen P, Schmugge T, Wilheit T T and Zwally H J 1976 Microwave emission from snow and glacier ice *J. Glaciol.* **16** 23–39

Cohen J 1994 Snow cover and climate *Weather* **49** 150–6

Eimers M C, Buttle J M and Watmough S A 2007 The contribution of rain-on-snow events to annual NO₃-N export from a forested catchment in south-central Ontario, Canada *Appl. Geochem.* **22** 1105–10

Foster J L *et al* 2011 A blended global snow product using visible, passive microwave and scatterometer satellite data *Int. J. Remote Sens.* **32** 1371–95

Grenfell T C and Putkonen J 2008 A method for the detection of the severe rain-on-snow event on Banks Island, October 2003, using passive microwave remote sensing *Water Resources Res.* **44** W03425

Hansen B B, Aanes R, Herfindal I, Kohler J and Saether B-E 2011 Climate, icing, and wild arctic reindeer: past relationships and future prospects *Ecology* **92** 1917–23

Hay L E and McCabe G J 2010 Hydrologic effects of climate change in the Yukon River Basin *Clim. Change* **100** 509–23

Karl T R, Melillo J M and Peterson T C 2009 *Global Climate Change Impacts in the United States* (Cambridge: Cambridge University Press)

Kattelmann R 1985 Macropores in snowpacks of Sierra Nevada *Annal. Glaciol.* **6** 272–3

Kidd R A, Bartsch A and Wagner W 2005 Development and validation of a diurnal difference indicator for freeze-thaw monitoring in the SIBERIA II project *ENVISAT and ERS Symposium (Salzburg, September 2004)* pp 2271–7 ESA SP-572

Kidd R A, Trommler M and Wagner W 2003 The development of a processing environment for time-series analysis of SeaWinds Scatterometer data *Int. Geosci. Remote Sens. Symp.* **6** 4110–2

Liston G E and Hiemstra C A 2011 The changing cryosphere: pan-arctic snow trends (1979–2009) *J. Clim.* **24** 5691–712

Long D and Brabets T 2002 *Coverage YUK.LAND and YUK.DEM National Stream Quality Accounting Network (NASQAN) Yukon River Basin, Canada and Alaska Landcover-Yukon River Basin* (Anchorage, AK: USGS)

Male D H and Granger R J 1981 Snow surface energy exchange *Water Resources Res.* **17** 609–27

Marks D and Dozier J 1992 Climate and energy exchange at the snow surface in the alpine region of the Sierra Nevada 2. Snow cover energy balance *Water Resources Res.* **28** 3043–54

Marks D, Kimball J, Tingey D and Link T 1998 The sensitivity of snowmelt processes to climate conditions and forest cover during rain-on-snow: a case study of the 1996 Pacific Northwest flood *Hydrol. Process.* **12** 1569–87

McCabe G J, Clark M P and Hay L E 2007 Rain-on-snow events in the Western United States *Bull. Am. Meteorol. Soc.* **88** 319–28

Mesinger F *et al* 2006 North American regional reanalysis: a long-term, consistent, high-resolution climate dataset for the North American domain, as a major improvement upon the earlier global reanalysis datasets in both resolution and accuracy *Bull. Am. Meteorol. Soc.* **87** 343–60

- Office of the Federal Coordinator for Meteorology (OFCM) 2005 *Federal Meteorological Handbook No.1, Surface Weather Observations and Reports* (FMH-1-2005) (available at www.ofcm.gov/fmh-1/fmh1.htm)
- Putkonen J and Roe G 2003 Rain-on-snow events impact soil temperatures and affect ungulate survival *Geophys. Res. Lett.* **30** 1188
- Putkonen J, Grenfell T C, Rennert K, Bitz C, Jacobson P and Russell D 2009 Rain on snow: little understood killer in the north *EOS Trans. Am. Geophys. Union* **90** 221–2
- Ramage J M, McKenney R A, Thorson B, Maltais P and Kopczynski S E 2006 Relationship between passive microwave-derived snowmelt and surface-measured discharge, Wheaton River, Yukon *Hydrol. Process.* **20** 689–704
- Rees A, Lemmetyinen J, Derksen C, Pulliainen J and English M 2010 Observed and modeled effects of ice lens formation on passive microwave brightness temperatures over snow covered tundra *Remote Sens. Environ.* **114** 116–26
- Rennert K J, Roe G, Putkonen J and Bitz C M 2009 Soil thermal and ecological impacts of rain on snow events in the circumpolar Arctic *J. Clim.* **22** 2302–15
- Schwartz M D, Ahas R and Aasa A 2006 Onset of spring starting earlier across the North Hemisphere *Glob. Change Biol.* **12** 343–51
- Serreze M C, Walsh J E, Chapin F S III, Osterkamp T, Dyurgerov M, Romanovsky V, Oechel W C, Morison J, Zhang T and Barry R G 2000 Observational evidence of recent change in the northern high latitude environment *Clim. Change* **46** 159–207
- Singh P, Spitzbart G, Hubl H and Weinmeister H W 1997 Hydrological response of snowpack under rain-on-snow events: a field study *J. Hydrol.* **202** 1–20
- Stone R S, Dutton E G, Harris J M and Longenecker D 2002 Earlier spring snowmelt in northern Alaska as an indicator of climate change *J. Geophys. Res.* **107** 4089
- Sverdrup H V 1936 The eddy conductivity of the air over a smooth snow field—results of the Norwegian-Swedish Spitzhergan Expedition in 1934 *Geophys. Publ.* **11** 1–69
- Ulaby F T, Moore R K and Fung A K 1986 *Microwave Remote Sensing: Active and Passive, Vol. III: From Theory to Applications* (Dedham, MA: Artech House)
- Wahrhaftig C 1965 *Physiographic Divisions of Alaska, Geological Survey Professional Paper 482* (Washington, DC: United States Government Printing Office)
- Wang L, Wolken G J, Sharp M J, Howell S E L, Derksen C, Brown R D, Markus T and Cole J 2011 Integrated pan-Arctic melt onset detection from satellite active and passive microwave measurements, 2000–2009 *J. Geophys. Res.* **116** D22103
- Westermann S, Boike J, Langer M, Schuler T V and Etzelmuller B 2011 Modeling the impact of wintertime rain events on the thermal regime of permafrost *Cryosphere Discuss.* **5** 1697–736
- Wilson R R, Bartsch A, Joly K, Reynolds J H, Orlando A and Loya W M 2012 Frequency, timing, extent, and size of winter thaw-refreeze events in Alaska 2001–2008 detected by remotely sensed microwave backscatter data *Polar Biol.* at press (doi:[10.1007/s00300-012-1272-6](https://doi.org/10.1007/s00300-012-1272-6))
- Woo M K, Thorne R, Szeto K and Yang D 2008 Streamflow hydrology in boreal region under the influences of climate and human interference *Phil. Trans. R. Soc. B* **363** 2251–60
- Ye H, Yang D and Robinson D 2008 Winter rain on snow and its association with air temperature *Hydrol. Process.* **22** 2728–36
- Yu P, Clausi D A and Howell S E L 2009 Fusing AMSR-E and QuikSCAT imagery for improved sea ice recognition *IEEE Trans. Geosci. Remote Sens.* **47** 1980–9
- Zuzel J F, Greenwalt R N and Allmaras R R 1983 Rain on snow: shallow, transient snowpacks with frozen soils *Proc. Western Snow Conf. 1983* pp 67–75 (Oregon State University Agricultural Experiment Station Technical Paper No. 6758)